

1 **Climate-driven legacies in simulated microbial communities alter litter decomposition rates**

2

3 Bin Wang^{1,2} and Steven Allison^{2,3}

4

5 1 Environmental Sciences Division, Oak Ridge National Laboratory, Oak Ridge, TN 37830 USA

6 2 Department of Ecology and Evolutionary Biology, University of California, Irvine, CA 92697

7 USA

8 3 Department of Earth System Science, University of California, Irvine, CA 92697 USA

9

10 **Abstract**

11 The mechanisms underlying diversity-functioning relationships have been a consistent area of
12 inquiry in biogeochemistry since the 1950s. Though these mechanisms remain unresolved in soil
13 microbiomes, many approaches at varying scales have pointed to the same notion—composition
14 matters. Confronting the methodological challenge arising from the complexity of microbiomes,
15 this study used the model DEMENTpy to explore trait-based drivers of microbiome-dependent
16 litter decomposition. We parameterized DEMENTpy for five sites along a climate gradient in
17 Southern California, USA, and conducted reciprocal transplant simulations analogous to a prior
18 empirical study. The simulations demonstrated climate-dependent legacy effects of microbial
19 communities on plant litter decomposition across the gradient. This result is consistent with the
20 previous empirical study across the same gradient. An analysis of community-level traits further
21 suggests that a 3-way tradeoff among resource acquisition, stress tolerance, and yield strategies
22 influences community assembly. Simulated litter decomposition was predictable with two
23 community traits (indicative of two of the three strategies) plus local environment, regardless of

24 the system state (transient versus equilibrium). If DEMENTpy predictions can be confirmed by
25 empirical studies, community traits plus local environmental factors (e.g., environment and litter
26 chemistry) may robustly predict litter decomposition across spatial-temporal scales. In conclusion,
27 this study offers a potential trait-based explanation for climate-dependent community effects on
28 litter decomposition with implications for improved understanding of whole-ecosystem
29 functioning across scales.

30

31 **Keywords:** microbiome, composition, decomposition, trait, tradeoff, climate, litter, history,
32 dispersal, legacy

33

34 1. Introduction

35 Understanding how ecosystems function across spatial-temporal scales often requires
36 knowledge of biotic community composition. This composition-functioning relationship has been
37 a consistent theme since the 1950s (**Harper 1967**). From terrestrial to aquatic to marine systems,
38 species composition has been quantified and related to systems functioning (e.g., **Loreau 2000**;
39 **Tilman et al. 2014**). Given that microbiomes comprise tremendous diversity and complexity in
40 the biosphere (e.g., **Bardgett and van der Putten, 2014; Tedersoo et al. 2014; Thompson et al.**
41 **2017**), understanding how microbiomes drive composition-functioning relationships can therefore
42 inform how entire ecosystems function.

43 Many efforts have addressed composition-functioning relationships in microbiomes, but
44 there are still unresolved mechanisms. For instance, functioning may saturate with increasing
45 microbial diversity (e.g., CO₂ production; **Yu et al. 2019**). Lab incubations of natural communities
46 showed that composition matters for rates of plant litter decomposition (e.g., **Strickland et al.**

47 2009; Cleveland et al. 2014). Similarly, field sampling and subsequent lab incubations under the
48 same conditions also revealed compositional effects (Rivett and Bell, 2018; Pascual-García and
49 Bell 2020).

50 In addition to varying community composition, there are studies that also manipulate local
51 environment to study community-environment interactions. For instance, Allison et al. (2013)
52 conducted a reciprocal transplant under varying drought and nitrogen deposition conditions in a
53 grassland ecosystem and found that changes in microbial community composition can indirectly
54 affect litter decomposition. In a gradient of lake sediments, Orland et al. (2019) showed that
55 community structure and environment interacted to influence CO₂ production. Notably,
56 overcoming some limitations in these earlier studies, Glassman et al. (2018) conducted a large
57 reciprocal transplant study across a climate gradient in Southern California, USA, and found
58 climate-dependent compositional effects on litter decomposition. Still, even in that study, the
59 mechanistic relationship between microbiome composition and functioning remained elusive.

60 The challenge of identifying underlying mechanisms may arise from interrelated
61 conceptual and methodological issues in the fields of microbial ecology and biogeochemistry. First,
62 many litter decomposition studies de-emphasize the role of microbial composition in controlling
63 soil carbon dynamics (e.g., Beugnon et al. 2021). This approach reflects the influential conceptual
64 framework of hierarchical control of litter decomposition (e.g., Lavelle et al. 1993; Aerts 1997).
65 That is, litter decomposition is argued to be hierarchically controlled by climate, substrate, and
66 microorganisms, with microbial community composition occupying the least important position.
67 More recently, this hierarchical theory has been challenged with the argument that decomposers
68 control litter decomposition beyond the local scale and that a more explicit consideration of
69 microbial communities is warranted (Bradford et al. 2017). Second, a high degree of functional

70 redundancy in soil microbiomes introduces methodological issues (**Finlay et al. 1997; Allison**
71 **and Martiny 2008**). Communities with different taxonomic composition can be functionally very
72 similar (**Louca et al. 2016**), making taxonomy-based approaches less relevant for predicting
73 ecosystem processes. These issues are probably the major contributors to the current
74 underappreciation of composition in modelling litter and soil organic matter decomposition (e.g.,
75 **Adair et al. 2008; Bradford et al. 2017**).

76 An alternative, emerging framework focuses on community-level functional traits that
77 mediate the composition-functioning relationship in microbial systems under various disturbances.
78 Trait-based investigations have been established in vegetation, showing clear advantages in
79 revealing community composition-function relationships (e.g., **McGill et al. 2006**). For instance,
80 recent studies demonstrated that traits can predict the long-term functional consequences of
81 biodiversity change, together with data on interacting abiotic factors (e.g., **van der Plas et al. 2020;**
82 **Klimešová et al. 2021; Wolf et al. 2021**). Trait-based quantification of microbial community
83 composition, especially considering high functional redundancy (e.g., **Allison and Martiny 2008;**
84 **Fetzer et al. 2015**), holds promise for distinguishing functioning between communities. **Malik et**
85 **al. (2020)** proposed a trait-based Y-A-S framework, arguing microbial communities trade off
86 among three primary strategies—Yield (Y), Acquisition (A), and Stress tolerance (S). Based on
87 this Y-A-S theory, under drought pressure, microbiomes were revealed to trade off resource
88 acquisition for stress tolerance (**Wang and Allison 2021**). Therefore, we hypothesize that
89 coordinated changes among traits representative of these three primary strategies may provide a
90 unifying explanation for composition-function relationships under environmental change.

91 Trait-based modelling offers a flexible framework in which processes and factors
92 influencing microbiomes' dynamics and functioning can be incorporated and easily manipulated.

93 The modeling approach circumvents some logistic and technical challenges currently facing
94 empirical studies. Following up on a previous reciprocal transplant experiment across a climate
95 gradient in Southern California, USA (**Glassman et al. 2018**), we explored trait-based mechanisms
96 with DEMENTpy, a trait-based microbial systems modelling framework (**Allison 2012; Wang**
97 **and Allison 2021**). Expanding an earlier modelling study focused on drought legacy in a grassland
98 ecosystem (**Wang and Allison 2021**), simulating the reciprocal transplant design allowed us to
99 disentangle the influence of compositional legacy versus local environment and their interactions
100 on litter decomposition while identifying the roles of community traits in mediating microbial
101 decomposition. A perturbation may affect microbiome functioning by altering community-level
102 traits through selection on different community-level strategies (e.g., **Watt 1947; Wilson 1997;**
103 **Whitham et al. 2006**). Guided by the overarching question of how microbial composition affects
104 litter decomposition, this modelling study specifically addressed the following specific questions:
105 1) What are the relative contributions of microbiome composition (legacy effects) versus local
106 environment to litter decomposition? 2) Similarly, what are their relative contributions to the
107 community-level traits of enzyme investment and drought tolerance? How are these traits
108 coordinated? And 3) How do community traits relate to litter decomposition?

109

110 **2 Methods**

111 **2.1 DEMENTpy**

112 DEMENTpy (Decomposition Model of Enzymatic Traits in Python) is a spatially explicit,
113 trait-based, microbial systems modelling framework built on top of an individual-based modelling
114 scheme (GitHub Repo: <https://github.com/bioatmosphere/DEMENTpy>; **Wang and Allison 2021**).
115 This model simulates microbial systems' dynamics in composition (in terms of hypothetical taxa)

116 and functioning (in terms of litter decomposition). Community dynamics are simulated by
117 explicitly modeling demographic processes of cell metabolism and growth, mortality, and
118 reproduction for each taxon population at a daily time step driven by daily temperature and litter
119 water potential. With explicit intra-cellular metabolism, microbial taxa secrete exoenzymes and
120 produce osmolytes both constitutively and inducibly. The exoenzymes degrade different organic
121 compounds at rates that depend on temperature and moisture. The production of osmolytes
122 depends on water potential, which confers drought tolerance. This model and its earlier versions
123 have been successfully applied to addressing a series of issues in microbial ecology (e.g., **Allison**
124 **2012; Allison and Goulden 2017; Wang and Allison 2019; Wang and Allison 2021**).

125

126 **2.2 Simulation of reciprocal transplanted microbiomes across a climate gradient**

127 Five sites representing five biomes (Desert, Scrubland, Grassland, Pine-Oak, and
128 Subalpine) were studied in Southern California, USA, forming a climate gradient spanning nearly
129 2,000 m of elevation and 15 °C of soil temperature (**Glassman et al. 2018**). More detailed
130 information about location, mean climate, and soil of these five sites can be found in **Supporting**
131 **Fig. 1** and the section on **Gradient Information** in the **Appendix**. A reciprocal transplant
132 simulation like the field study by **Glassman et al. (2018)** was conducted with DEMENTpy across
133 this gradient following a ‘transplant’ protocol as follows.

134 Prior to transplant, we conducted a 3-year spin-up to equilibrate microbiomes with site-
135 specific litter and climate at each of the five sites (**Wang and Allison 2021**). One year of climate
136 data from 2011 (representative of normal meteorological conditions) was recycled three times at
137 each site. At year four, simulated microbiomes ($n = 20$ per site) were designated as the starting
138 communities for transplantation. These microbiomes were initiated on grassland litter and

139 reciprocally ‘transplanted’ to the five sites where they were exposed to site-specific climate forcing,
140 mimicking the empirical design (**Glassman et al. 2018**). These ‘transplant’ simulations lasted four
141 years with each transplant corresponding to a spin-up [$n = 100$ per site (5 community x 20 spin-
142 ups)].

143 With this transplant simulation protocol, we ran two different forcing scenarios. One
144 scenario recycled the 2011 climate forcing through 8 years of simulations (hereafter referred to as
145 average forcing; **Supporting Fig.2**). Another recycled the 2011 forcing for three years to reach
146 equilibrium, then following the field transplant timeline, used 2015 forcing before the transplant
147 and 2016-2019 forcing after the transplant (hereafter referred to as actual forcing; **Supporting**
148 **Fig.3**). The average forcing scenario was intended to emphasize the effect of site-driven climate
149 variation on microbial legacies and to speed up the system return to equilibrium, whereas the actual
150 forcing overlays a greater range of natural climate variability that slows the system return to
151 equilibrium following transplantation, as in the Glassman et al. experiment. Daily soil surface
152 temperature (°C) for each site was derived from averaging field soil temperature measurements
153 for the average forcing and approximated using the Daymet (version 4; **Thornton et al. 2020**)
154 daily temperature product for actual forcing. Estimates of litter water potential (MPa) were derived
155 from analysis of fuel moisture sensors at the grassland site, near Loma Ridge, California (**Allison**
156 **and Goulden 2017**) using two different scaling methods for the average and actual forcing,
157 respectively. See section **DEMENTpy forcing** in the **Appendix** for details.

158 All transplant scenarios were initialized on a 100 by 100 spatial grid with a bacterial
159 community of 100 hypothetical taxa using well-informed parameter values (see parameter values
160 in **Allison and Goulden 2017; Wang and Allison 2021**). The pool of taxa was the same prior to
161 spin-up at all five sites. Leaf litter concentrations of C-, N-, and P-containing substrates (mg cm^{-3})

162 were estimated based on near-infrared spectroscopy measurements at each site along the climate
163 gradient (**Baker and Allison 2017**). Within each forcing scenario, we ran ensembles of 20
164 independent simulations (corresponding to 20 independent spin-ups) for each transplant
165 combination (5 sites x 5 communities x 20 spin-ups = 500). Each of the 25 combinations used the
166 same set of 20 seeds for random number generation.

167

168 **2.3 Data analyses**

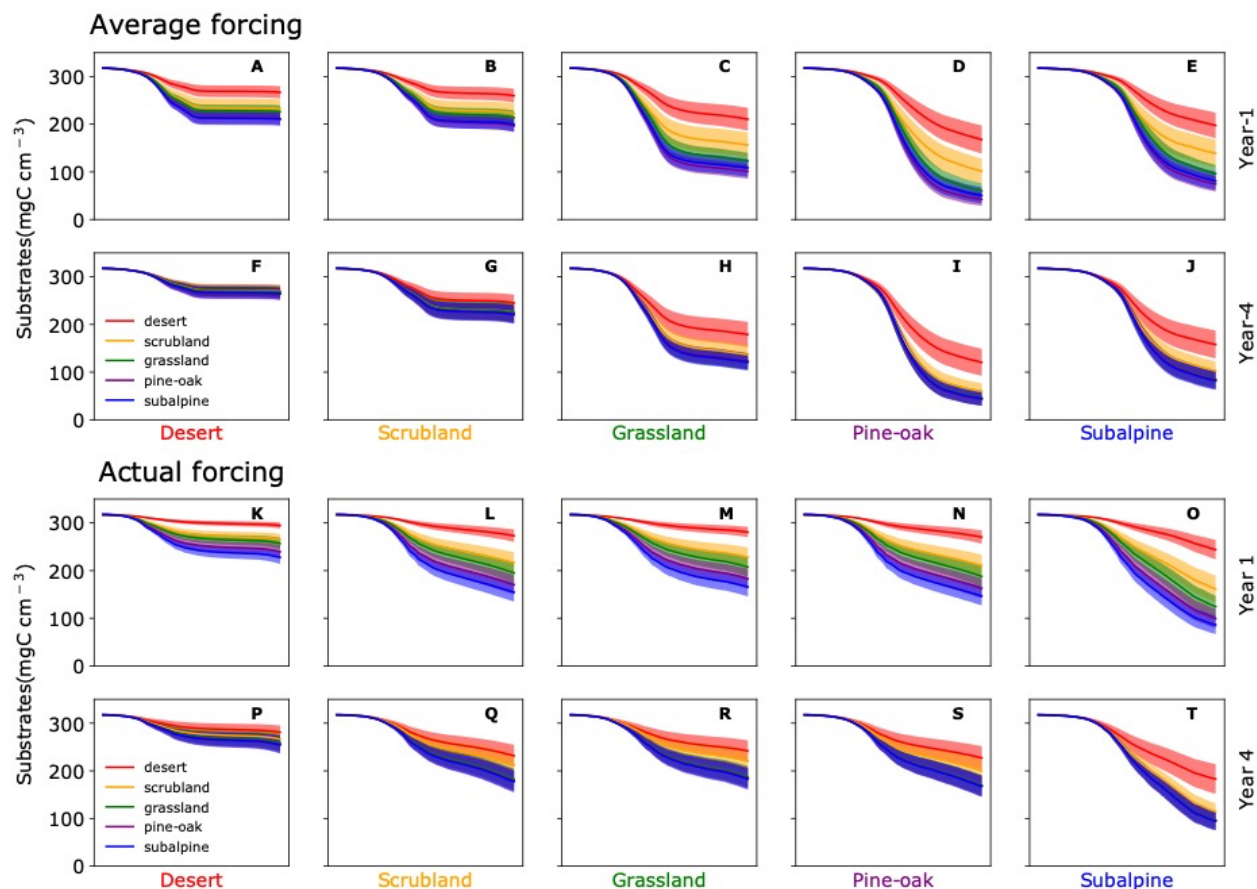
169 We analyzed simulation outputs for litter mass loss (i.e., total substrate remaining) and
170 community-level traits (enzyme investment, and drought tolerance) as well as community-level
171 allocation to enzymes, osmolytes, and yield. Enzyme investment and drought tolerance are
172 biomass-weighted community mean trait values. Using site-specific temperature and water
173 potential, a series of statistical analyses were performed on these data (with R v4.1). First, variance
174 partitioning of decomposition (i.e., total substrate remaining) among factors of community (i.e.,
175 origin) and site (i.e., local environment), as well as their interactions was conducted with two-way
176 ANOVA. The same analysis was performed twice to further test whether system state (transient:
177 the end of the 1st year; equilibrium: the end of the 4th year under the average forcing) was a factor
178 contributing to the changes in decomposition. Similarly, to disentangle factors influencing
179 community enzyme investment and drought tolerance (an advantage of this modelling study),
180 variance partitioning of enzyme investment and drought tolerance with two-way ANOVA was
181 performed. Again, the same analysis was performed at two different time points in different years.
182 Furthermore, Pearson's correlation was used to examine relationships between the two traits. To
183 test whether community traits can explain decomposition, a series of four multiple linear
184 regressions of decomposition against covariates of local environment (temperature and water

185 potential), enzyme investment, and/or drought tolerance were performed with the least-squares
186 approach. These multiple linear regression models were fitted separately to the 1st year and the 4th
187 year data (including annual litter decomposition and mean traits and temperature and water
188 potential) pooled together from all five sites. Adjusted R² and information criteria of AIC and more
189 parsimonious BIC were used to evaluate model performance. Assumptions of normality and
190 equality of variance were ensured to be met during the analysis.

191

192 3. Results

193 3.1 Partitioning variance of litter decomposition



194

195 **Fig. 1 Decomposition across the gradient during the 1st year and 4th year after transplant**
196 **under both average forcing (A-J) and actual forcing (K-T).** The color band is 90% confidence
197 interval (n=20).

198

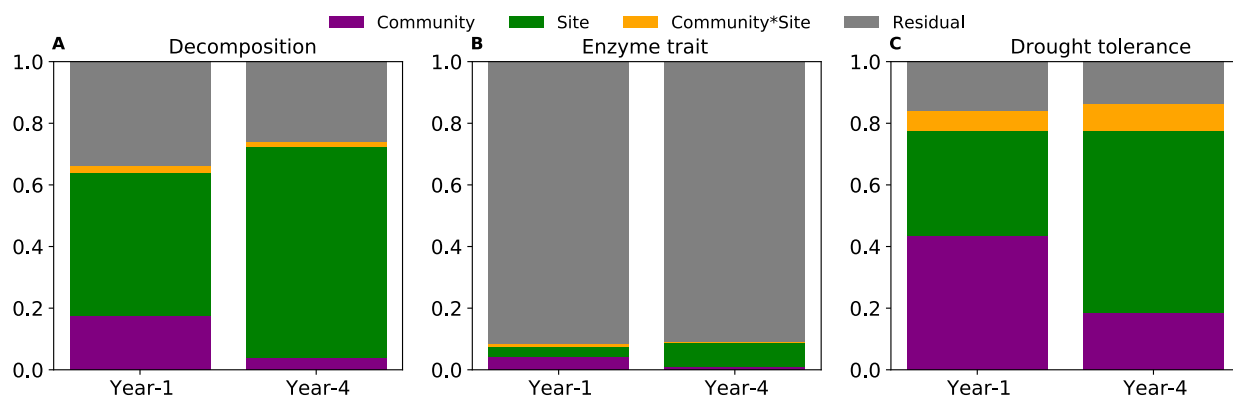
199 After the spin-up and before transplant, different microbial communities were realized
200 across the gradient as indicated by differences in community traits of enzyme investment and
201 drought tolerance (**Supporting Fig. 4**). Overall, from desert to subalpine, the drought tolerance
202 decreased while the enzyme investment increased under both average forcing and actual forcing.
203 However, this overall pattern was less pronounced for enzyme investment than for drought
204 tolerance, especially for enzyme investment under average forcing (**Supporting Fig. 4B**).

205 In the 1st year after transplantation, the five communities showed different litter-
206 decomposing capability across the gradient (**Fig. 1**). These differences were mainly consistent
207 between average forcing and actual forcing (**Fig. 1**). Decomposition was strongly influenced by
208 local environment, with a pronounced increase (i.e., less substrate remaining) from desert to
209 subalpine sites ($df = 4$, $P < 0.001$). The microbial community significantly affected decomposition
210 as well ($df = 4$, $P < 0.001$), with the desert community overall decomposing the least and the pine-
211 oak and subalpine communities decomposing the most with average forcing. With actual forcing,
212 the subalpine community consistently decomposed the most. However, this community effect
213 varied with local conditions (significant community by site interaction; $df = 16$; $P < 0.05$). The
214 pattern of community differences was comparable across the desert and scrubland sites, but distinct
215 from the other three sites. Particularly for the average forcing, those other three sites differentiated
216 the five communities more strongly than the desert and scrubland sites.

217 By the 4th year after transplant, decomposition in the average and actual forcing scenarios
218 became much more similar across the five sites (Year 4 in **Fig. 1**). Though community ($df = 4$, $P <$
219 0.001) and its interaction with local conditions ($df = 16$, $P < 0.05$) were still statistically significant,
220 only the desert community at the pine-oak and subalpine sites remained significantly different
221 from the other communities (and only the subalpine site under actual forcing). All the other
222 communities, especially at the desert and scrubland sites, showed similar litter decomposition.

223 The change in decomposition over time from the 1st through the 4th year was reflected in
224 the changing relative contribution of community, local environment, and their interactions to the
225 variance of litter decomposition. Take the average forcing case for example (**Fig. 2**). After the 1st
226 year, community, local environment, and their interactions accounted for 17.6 %, 46.4 %, and 2.0 %
227 of the variance in decomposition. By contrast, by the end of the 4th year, the contribution from
228 community sharply declined to only about 3.8% (the interaction to 1.5%), and local environment
229 increased to about 68.6%.

230

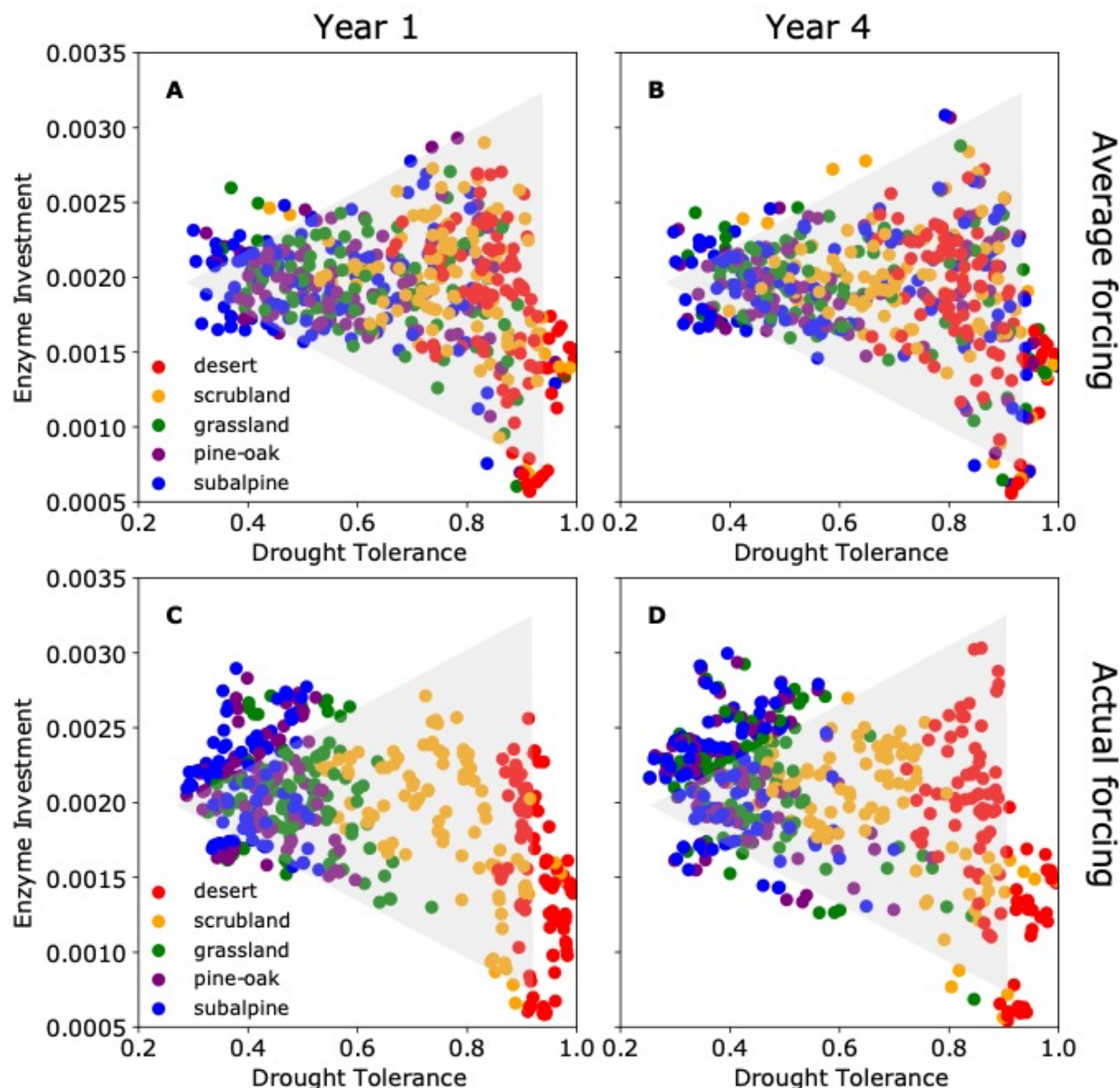


231
232 **Fig. 2 Variance partitioning of decomposition (A), enzyme trait (B), and drought tolerance**
233 **(C)**. For enzyme trait (B) only community and site are significant in year 1, and only site is
234 significant in year 4.

235

236 **3.2 Changes in coordination of community-level traits**

237



238

239 **Fig. 3 Enzyme investment versus drought tolerance by the end of year 1 and year 4 after the
240 transplant.** A and B are under the average forcing, while C and D are under the actual forcing.

241 The equilateral triangles in grey are the same across the panels. Data are pooled together across
242 the gradient and color-coded by site.

243

244 Meanwhile, the relative differences in traits between the communities changed from the 1st
245 through the 4th year (**Fig. 2B, C**). After the 1st year, 4.4% of the variance in the enzyme trait was
246 attributed to community ($df = 4$; $P < 0.001$) and 3.0% was attributed to local environment ($df = 4$;
247 $P < 0.01$). However, after the 4th year, the enzyme trait was only significantly influenced by local
248 environment ($df = 4$; $P < 0.001$), which explained only 7.6% of the variance. By contrast, the
249 drought trait was consistently and significantly affected by community ($df = 4$; $P < 0.001$), local
250 environment ($df = 4$; $P < 0.001$), and their interaction ($df = 4$; $P < 0.001$), though the relative
251 contribution from community and local environment decreased (43.6% to 18.5%) and increased
252 (34.0% to 59.2%), respectively, from the 1st to the 4th year. The contribution from their interactions
253 increased slightly (6.5% to 8.4%).

254 Even with these changes in community traits, enzyme investment and drought tolerance
255 across the gradient were consistently confined to an identical triangular space without changing
256 over time under both the average forcing and actual forcing (**Fig. 3**). This distribution held even
257 though the traits displayed varying correlations in different sites across the gradient (**Supporting**
258 **Fig. 5**). Overall, these two traits were negatively correlated among the five communities both
259 across the gradient and over time. At both time points, the correlation strength displayed an overall
260 descending pattern across the gradient from low to high elevation. In addition, although the
261 strength by the end of the 4th year was overall lower than the 1st year across the sites, it is
262 noteworthy that the desert site did not change (**Supporting Fig. 5F**), and that the subalpine site

263 became uncorrelated (**Supporting Fig. 5J**). These changes in traits and their correlations dictated
264 community-level resource allocation among enzymes, osmolytes, and yield (**Supporting Fig. 6**).

265

266 **3.3 Relating community traits to litter decomposition**

267

268 **Table 1. Regression models predicting annual litter decomposition as a linear function of**
269 **temperature, water potential, enzyme investment trait, and/or drought tolerance trait.**

Model	Year 1 (Transient)			Year 4 (Equilibrium)		
	Adjusted R ²	AIC	BIC	Adjusted R ²	AIC	BIC
Model 1 <i>f(temp, psi)</i>	0.43	5565.28	5582.24	0.66	5410.42	5427.28
Model 2 <i>f(temp, psi, enz)</i>	0.67	5297.44	5318.51	0.76	5232.42	5253.50
Model 3 <i>f(temp, psi, drt)</i>	0.59	5405.83	5426.90	0.71	5328.41	5349.48
Model 4 <i>f(temp, psi, enz, drt)</i>	0.74	5183.35	5208.64	0.79	5172.56	5197.84

270

271 Community traits were related to annual decomposition with four multiple linear regression
272 models (**Table 1**). In the 1st year, a model with either enzyme investment (Model 2) or drought
273 tolerance traits (Model 3) explained decomposition better than a model with only local temperature
274 and moisture (Model 1). Although Model 2 with enzyme investment was better than Model 3 with
275 drought tolerance, only Model 4 with both drought tolerance and enzyme investment outperformed

276 all three other models (both the smallest AIC and BIC and the largest adjusted R² values). The
277 performance of Model 4 was the best as well in the 4th year (both the smallest AIC and BIC and
278 the largest adjusted R² values), though its margin over Model 2 with enzyme investment was
279 relatively small. In combination, a model with both enzyme and drought tolerance traits had the
280 strongest explanatory power.

281

282 **4.Discussion**

283 Identifying the mechanisms underpinning microbiomes' composition-functioning
284 relationship is a research theme of fundamental importance but with methodological challenges.
285 Our study approached this issue from a trait-based perspective using the theory-driven trait-based
286 microbiome model—DEMENTpy—complemented by statistical modelling analyses. Overall, our
287 simulations of litter decomposition were consistent with a previous transplant experiment in that
288 both studies found evidence for climate-dependent legacy effects of microbial community
289 composition (**Glassman et al. 2018**). Our model analysis of community-level traits further
290 suggests that a 3-way tradeoff may mediate these legacies and the effects of local environment on
291 community composition.

292

293 **4.1 Comparison with empirical study**

294 This modelling study agrees with the general conclusion of the earlier field transplant
295 experiment by **Glassman et al. (2018)** that microbial composition matters in climate-dependent
296 litter decomposition. In both studies, transplanted communities reflected the legacy of
297 environmental conditions in their ecosystems of origin (including temperature, precipitation, and
298 litter chemistry). Broadly speaking, model-predicted compositional effects and interactions

299 between the community and local environment (**Fig. 1**) were consistent with the field experiment.
300 Moreover, the relative contributions of community, local environment, and their interactions to the
301 variance in decomposition were also similar in both studies. Within 6 to 18 months after the
302 transplant, **Glassman et al. (2018)** reported ranges of these contributions of ~6-10% for the
303 community (vs 17.6% for the simulations at one year after transplant), ~30 - 65% (vs 46.4%) for
304 local environment, and no significance to a maximum of 19% (vs 2.0%) for their interactions. In
305 accordance with the empirical results that showed an increasing contribution from local
306 environment over time, our modelling study also revealed that the legacy effects of composition
307 declined over time, albeit at a longer timescale of four years (**Fig.2A**).

308 Although **Glassman et al (2018)** found evidence for community-driven difference in litter
309 decomposition, they did not find significant support for Home Field Advantage (HFA; **Gholz et**
310 **al. 2000; Veen et al. 2018**) within a measurement time frame of 6 to 18 months after the transplant.
311 Similarly, in our modelling study, by the end of the 1st year, the average decomposition of the five
312 communities was very close to each other in the desert site (under both the average forcing and
313 actual forcing), and the subalpine community had the most decomposition under actual forcing
314 (though not significantly different) and relatively high decomposition under average forcing (not
315 significantly different as well; **Fig. 1**). Moreover, whether the system reached equilibrium in the
316 4th year (under the average forcing) or not (under the actual forcing), all HFA disappeared (**Fig.1**).
317 Therefore, our modelling results and the field investigation were comparable, although the time
318 scale was different.

319 Though differing from Glassman et al.'s transplant experiment in some details, our
320 modelling work confirms the empirical result that litter decomposition depends on microbial
321 community composition. This finding adds to an increasing body of evidence along similar lines

322 (e.g., **Strickland et al. 2009; Allison et al. 2013; Cleveland et al. 2014; Bradford et al. 2017;**
323 **Zakem et al. 2021**). Moreover, some legacy effects may persist and thus cause different
324 functioning under the same conditions (**Wang and Allison 2021**). Such persistence is widely
325 observed across different natural systems (e.g., **Ortiz et al. 2020; Wilson et al. 2021**). Although
326 dispersal in soil microbiomes may counter persistence (**Wang and Allison 2021**), these results
327 underscore the nonnegligible role of environmental history as a key factor in litter decomposition
328 (**Spencer 2020**).

329

330 **4.2 Co-ordination of community traits**

331 The notion of multidimensional tradeoffs in the biosphere is increasingly being embraced
332 as organisms evolve across organizational and spatial-temporal scales under physical, biological,
333 and ecological constraints (e.g., **Kempes et al. 2019**). Trait-based quantification of communities
334 provides an approach for identifying those tradeoffs. Most notably, rich data on plant traits have
335 revealed multidimensional tradeoffs first in shoots (e.g., **Díaz et al. 2016**), then in roots (e.g.,
336 **Weemstra et al. 2016**), and more recently in whole plants (**Weigelt et al. 2021**). Using these traits,
337 vascular plants can be classified into the CSR (Competitor, Stress-tolerator, Ruderal) strategy
338 scheme (**Pierce et al. 2017**). The same approach applies to multi-tradeoffs in phytoplankton
339 (**Edwards et al. 2011**) and animals (**De Froment et al. 2014**). Our modelling study suggests there
340 are also multi-dimensional tradeoffs in soil microbial communities. In particular, tradeoffs among
341 enzyme investment, drought tolerance, and yield determine the microbial response to climate
342 disturbance (**Fig. 3; Supporting Fig. 6**).

343 Dispersal is another key process influencing community assembly, which itself can be
344 shaped by local conditions and stochasticity (e.g., order of taxa arrival; **Fukami 2015; Reijenga**

345 et al. 2021). Our earlier study revealed that rapid dispersal could counter legacy effects driven by
346 changes in microbial composition (Wang and Allison 2021). Potentially many other disturbances
347 (e.g., fire and nitrogen deposition) can combine to shape microbial community strategies. To tease
348 out how each of these factors and their interactions drive 3-way tradeoffs in community traits,
349 additional efforts focused on specific factors of interest are needed (e.g., Coyte et al. 2021).

350

351 **4.3 A unifying framework of trait-based prediction of litter decomposition?**

352 Our analysis suggests that litter decomposition rates can be predicted with at least two
353 community traits plus local environmental conditions (Table 1). This analysis contrasts with the
354 assumption that community composition makes a negligible contribution to litter decomposition
355 (Adair et al. 2008; Lavelle et al. 1993; Aerts 1997; Bradford et al. 2017). Moreover, our model
356 provides a useful approach for predicting decomposition across spatial-temporal scales that can
357 integrate effects of past disturbances. Such an approach is important as empirical studies of litter
358 decomposition and soil carbon stocks move beyond snapshots of large-scale spatial data to include
359 information on disturbance and recovery (Bradford et al. 2021). However, this approach points
360 to a challenge of measuring and deriving traits empirically.

361

362 **4.4 Measuring and simulating community traits more accurately**

363 Our modeling framework, though promising, still needs to confront the challenge of
364 parameterizing microbial traits based on empirical data. Uncertainty remains in the simulated
365 community traits due to missing processes such as fungi-bacteria interactions (e.g., Wright and
366 Vetsigian 2016), realistic dispersal (e.g., Cunillera - Montcusí et al. 2021), and evolution.
367 Notably, a recent study across the Glassman et al. climate gradient found fast bacterial evolution

368 in addition to ecological adaptation (**Chase et al. 2021**). This fast evolution, plus ecological drift
369 resulting from fluctuating population sizes due to chance events (e.g., **Travisano et al. 1995**), can
370 cause differences in community trait composition. Representing these processes in DEMENTpy
371 may help make the predicted shifts in trait-based strategies more accurate.

372 Making these model improvements will require more empirical measurements of traits.
373 Our simulations assume that enzymes and osmolytes are the main metabolites driving Y-A-S
374 tradeoffs. However, microbes have complex metabolic networks, suggesting that many more traits
375 are involved in Y-A-S strategies (**Malik et al. 2020**). These additional traits (e.g., **Weisskopf et**
376 **al. 2021**) may still fit in the 3-way tradeoff framework, but new techniques are needed to translate
377 trait measurements into the parameters used by DEMENTpy to predict litter decomposition. A
378 promising, yet challenging, approach would be to derive indices of stress tolerance versus resource
379 allocation traits from rich -omics data (e.g., **Malik et al. 2020; Monson et al. 2021; Heinken et**
380 **al. 2021**) using machine learning techniques (e.g., **Chen et al. 2021**).

381

382 **4.5 Broader implications for understanding whole-ecosystem functioning**

383 Our findings are applicable to improved prediction of whole ecosystem functioning. For
384 example, incorporating plant-microbiome interactions into such predictions has been challenging
385 (e.g., **Van Voris et al. 1980; Ramirez et al. 2020**), but our modeling approach provides a starting
386 point. Litter chemistry, which can be associated with above- and below-ground plant traits
387 (**Cornwell et al. 2008**), clearly influences litter decomposition. Therefore, it could be fruitful to
388 predict litter decomposition at large scales by linking plant and microbial traits. Such an approach
389 could even allow simultaneous consideration of legacy effects on vegetation and microbial
390 communities, as well as their interaction (e.g., **Schmid et al. 2021**).

391 More generally, our study, together with recent vegetation modelling (e.g., **Wang et al.**
392 **2018; Rüger et al. 2020**), suggests model predictions could be improved by considering the multi-
393 dimensional nature of trait tradeoffs in microbiomes and the biosphere in general. Vegetation
394 modeling is already moving in this direction (e.g., **Kraft et al. 2015; Bruelheide et al. 2018;**
395 **Weigelt et al. 2021**), and microbiome studies are catching up (**Westoby et al. 2021**). Still, there
396 remains the challenge of incorporating these multidimensional tradeoffs into ecosystem and Earth
397 system models (e.g., **Fiedler et al. 2021; Terrer et al. 2021**) while avoiding the computational
398 expense of simulating microbial and vegetation composition locally. Informing larger-scale
399 models with outputs from trait-based community models, either through direct or offline coupling,
400 may be a potential way forward.

401

402 **5. Conclusions**

403 Our theory-driven modelling study suggests that climate-dependent changes in litter
404 decomposition depend on shifts in microbial functional strategies within a 3-way tradeoff space.
405 These shifts integrate legacies of past disturbance as a key driver of decomposition. Emerging
406 from these findings is a framework for predicting microbial litter decomposition as a function of
407 at least two community-level traits interacting with local climate and litter substrate. This
408 framework implies that a data-driven statistical model could predict litter decomposition and soil
409 organic matter dynamics if high-quality empirical measurements of community traits are available
410 at sufficient temporal resolution. Our work also suggests that trait-based modelling, together with
411 progress made in trait-based vegetation studies, is an effective tool for exploring the mechanisms
412 underlying ecosystem functioning in the context of disturbance. These tools should be applied to
413 understand the roles of microbiomes in the functioning of the Earth system. Overall, our study

414 sheds light on the mechanisms underpinning the diversity-functioning relationship in complex
415 microbiomes.

416

417 **Acknowledgements**

418 The version of DEMENTpy used in this study is available at
419 <https://github.com/bioatmosphere/DEMENTpy>. Data and code underlying the analyses of this
420 manuscript are publicly available in this GitHub
421 Repository:<https://github.com/bioatmosphere/microbiome-climate-gradient>. This research used
422 resources of the Compute and Data Environment for Science (CADES) at the Oak Ridge National
423 Laboratory, which is supported by the Office of Science of the US Department of Energy (DOE)
424 under Contract No. DE-AC05-00OR22725. Funding was provided by the US DOE, Office of
425 Science, Biological and Environmental Research award DE-SC0020382, and the US National
426 Science Foundation award DEB-1457160.

427

428 **References**

- 429 Adair EC, et al. (2008) Simple three-pool model accurately describes patterns of long-term litter
430 decomposition in diverse climates. *Global Change Biology*, 14, 2636–2660
- 431
- 432 Aerts, R. (1997). Climate, leaf litter chemistry and leaf litter decomposition in terrestrial
433 ecosystems: a triangular relationship. *Oikos*, 439-449.
- 434
- 435 Allison, S. D. 2012. A trait-based approach for modelling microbial litter decomposition. *Ecology*
436 Letters 15: 1058– 1070.

- 437
- 438 Allison, S. D., and M. L. Goulden. 2017. Consequences of drought tolerance traits for microbial
439 decomposition in the DEMENT model. *Soil Biology and Biochemistry* 107: 104– 113.
- 440
- 441 Allison, S. D., Y. Lu, C. Weihe, M. L. Goulden, A. C. Martiny, K. K. Treseder, and J. B. Martiny.
442 2013. Microbial abundance and composition influence litter decomposition response to
443 environmental change. *Ecology* 94: 714– 725.
- 444
- 445 Allison, S. D., and J. B. Martiny. 2008. Resistance, resilience, and redundancy in microbial
446 communities. *Proceedings of the National Academy of Sciences of the United States of America*
447 105: 11512– 11519.
- 448
- 449 Baker, N. R., & Allison, S. D. (2017). Extracellular enzyme kinetics and thermodynamics along a
450 climate gradient in southern California. *Soil Biology and Biochemistry*, 114, 82-92.
- 451
- 452 Bardgett, R., van der Putten, W. (2014). Belowground biodiversity and ecosystem functioning.
453 *Nature* 515, 505–511
- 454
- 455 Beugnon, R., Du, J., Cesarz, S., Jurburg, S. D., Pang, Z., Singavarapu, B., ... & Eisenhauer, N.
456 (2021). Tree diversity and soil chemical properties drive the linkages between soil microbial
457 community and ecosystem functioning. *ISME Communications*, 1, 1-11.
- 458

- 459 Bradford, M.A., Wood, S.A., Addicott, E.T. et al. (2021). Quantifying microbial control of soil
460 organic matter dynamics at macrosystem scales. *Biogeochemistry* 156, 19–40.
- 461
- 462 Bruelheide, H., Dengler, J., Purschke, O. et al. (2018). Global trait–environment relationships of
463 plant communities. *Nature Ecology and Evolution* 2, 1906–1917.
- 464
- 465 Chen, L., Lu, W., Wang, L. et al. Metabolite discovery through global annotation of untargeted
466 metabolomics data. *Nat Methods* (2021). <https://doi.org/10.1038/s41592-021-01303-3>
- 467
- 468 Chen, Y., Liu, F., Kang, L., Zhang, D., Kou, D., Mao, C., ... & Yang, Y. (2021). Large-scale
469 evidence for microbial response and associated carbon release after permafrost thaw. *Global
470 Change Biology*. <https://doi.org/10.1111/gcb.15487>
- 471
- 472 Cleveland CC, et al. (2014) Litter quality versus soil microbial community controls over
473 decomposition: A quantitative analysis. *Oecologia* 174,283–294.
- 474
- 475 Cornwell, W. K., Cornelissen, J. H., Amatangelo, K., Dorrepaal, E., Eviner, V. T., Godoy, O., ...
476 & Westoby, M. (2008). Plant species traits are the predominant control on litter decomposition
477 rates within biomes worldwide. *Ecology Letters*, 11, 1065-1071.
- 478
- 479 Coyte KZ, Rao C, Rakoff-Nahoum S, Foster KR (2021) Ecological rules for the assembly of
480 microbiome communities. *PLoS Biol* 19, e3001116.
- 481

- 482 Cunillera-Montcusí, D., Borthagaray, A. I., Boix, D., Gascón, S., Sala, J., Tornero, I., ... & Arim,
483 M. (2021). Metacommunity resilience against simulated gradients of wildfire: disturbance
484 intensity and species dispersal ability determine landscape recover capacity. *Ecography*. 44, 1022–
485 1034
- 486
- 487 de Froment, A. J., Rubenstein, D. I., & Levin, S. A. (2014). An extra dimension to decision-making
488 in animals: the three-way trade-off between speed, effort per-unit-time and accuracy. *PLOS
489 Comput Biol*, 10, e1003937.
- 490
- 491 Díaz, S., Kattge, J., Cornelissen, J. H., Wright, I. J., Lavorel, S., Dray, S., ... & Gorné, L. D. (2016).
492 The global spectrum of plant form and function. *Nature*, 529, 167-171.
- 493
- 494 Eckburg, P. B., Bik, E. M., Bernstein, C. N., Purdom, E., Dethlefsen, L., Sargent, M., ... & Relman,
495 D. A. (2005). Diversity of the human intestinal microbial flora. *science*, 308, 1635-1638.
- 496
- 497 Edwards, K. F., Klausmeier, C. A., & Litchman, E. (2011). Evidence for a three-way trade-off
498 between nitrogen and phosphorus competitive abilities and cell size in phytoplankton. *Ecology*,
499 92, 2085-2095.
- 500
- 501 Fabian, J., Zlatanovic, S., Mutz, M. et al. (2017). Fungal–bacterial dynamics and their contribution
502 to terrigenous carbon turnover in relation to organic matter quality. *ISME J* 11, 415–425.
- 503

- 504 Fargione, J., Brown, C. S., & Tilman, D. (2003). Community assembly and invasion: an
505 experimental test of neutral versus niche processes. *Proceedings of the National Academy of*
506 *Sciences* 100, 8916-8920.
- 507
- 508 Fetzer, I., Johst, K., Schäwe, R., Banitz, T., Harms, H., & Chatzinotas, A. (2015). The extent of
509 functional redundancy changes as species' roles shift in different environments. *Proceedings of*
510 *the National Academy of Sciences* 112, 14888-14893.
- 511
- 512 Fiedler, S., Monteiro, J. A., Hulvey, K. B., Standish, R. J., Perring, M. P., & Tietjen, B. (2021).
513 Global change shifts trade-offs among ecosystem functions in woodlands restored for
514 multifunctionality. *Journal of Applied Ecology*. 58, 1705–1717
- 515
- 516 Finlay, B. J., Maberly, S. C., & Cooper, J. I. (1997). Microbial diversity and ecosystem function.
517 *Oikos*, 80, 209-213.
- 518
- 519 Gholz, H. L., Wedin, D. A., Smitherman, S. M., Harmon, M. E., & Parton, W. J. (2000). Long-
520 term dynamics of pine and hardwood litter in contrasting environments: toward a global model of
521 decomposition. *Global Change Biology*, 6, 751-765.
- 522
- 523 Harper, J. L. 1967. A Darwinian Approach to Plant Ecology. *Journal of Ecology*, 55, 247-270.
- 524
- 525 Heinken A, Basile A, Thiele I, Advances in constraint-based modelling of microbial communities,
526 Current Opinion in Systems Biology, <https://doi.org/10.1016/j.coisb.2021.05.007>.

- 527
- 528 Herzschuh, U. (2020). Legacy of the Last Glacial on the present-day distribution of deciduous 521
529 versus evergreen boreal forests. *Global Ecology and Biogeography*, 29, 198-206
- 530
- 531 John, M. G. S., Orwin, K. H., & Dickie, I. A. (2011). No ‘home’ versus ‘away’ effects of
532 decomposition found in a grassland–forest reciprocal litter transplant study. *Soil Biology and*
533 *Biochemistry*, 43, 1482-1489.
- 534
- 535 Kempes, C. P., Koehl, M. A. R., & West, G. B. (2019). The scales that limit: the physical
536 boundaries of evolution. *Frontiers in Ecology and Evolution*, 7, 242.
- 537
- 538 Klimešová, J., Mudrák, O., Martíková, J., Lisner, A., Lepš, J., Filartiga, A. L., & Ottaviani, G.
539 (2021). Are belowground clonal traits good predictors of ecosystem functioning in temperate
540 grasslands? *Functional Ecology*, 35, 787-795.
- 541
- 542 Kraft, N. J., Godoy, O., & Levine, J. M. (2015). Plant functional traits and the multidimensional
543 nature of species coexistence. *Proceedings of the National Academy of Sciences*, 112, 797-802.
- 544
- 545 Loreau, M. (2000). Biodiversity and ecosystem functioning: recent theoretical advances. *Oikos*,
546 91, 3-17.
- 547
- 548 Louca, S., Parfrey, L. W., & Doebeli, M. (2016). Decoupling function and taxonomy in the global
549 ocean microbiome. *Science* 353, 1272-1277.

- 550
- 551 Lavelle, P., Blanchart, E., Martin, A., Martin, S., & Spain, A. (1993). A hierarchical model for
552 decomposition in terrestrial ecosystems: application to soils of the humid tropics. *Biotropica* 25,
553 130-150.
- 554
- 555 Langenheder S, Bulling MT, Solan M, Prosser JI (2010) Bacterial Biodiversity-Ecosystem
556 Functioning Relations Are Modified by Environmental Complexity. *PLoS ONE* 5, e10834.
- 557
- 558 Lustenhouwer, N., Maynard, D. S., Bradford, M. A., Lindner, D. L., Oberle, B., Zanne, A. E., &
559 Crowther, T. W. (2020). A trait-based understanding of wood decomposition by fungi.
560 *Proceedings of the National Academy of Sciences*, 117, 11551-11558.
- 561
- 562 McGill, B. J., B. J. Enquist, E. Weiher, and M. Westoby. 2006. Rebuilding community ecology
563 from functional traits. *Trends in Ecology & Evolution* 21, 178–185.
- 564
- 565 Mille-Lindblom, C., & Tranvik, L. J. (2003). Antagonism between bacteria and fungi on
566 decomposing aquatic plant litter. *Microbial Ecology* 45, 173-182.
- 567
- 568 Orland, C., Emilson, E.J.S., Basiliko, N. et al. (2019). Microbiome functioning depends on
569 individual and interactive effects of the environment and community structure. *ISME J* 13, 1–11
- 570

- 571 Ortiz, Y., Restrepo, C., Vilanova-Cuevas, B., Santiago-Valentin, E., Tringe, S. G., & Godoy-
- 572 Vitorino, F. (2020). Geology and climate influence rhizobiome composition of the phenotypically
- 573 diverse tropical tree *Tabebuia heterophylla*. *PLoS One*, 15, e0231083.
- 574
- 575 Pascual-García, A., Bell, T. (2020). Community-level signatures of ecological succession in
- 576 natural bacterial communities. *Nature Communications*, 11, 2386.
- 577
- 578 Pierce, S., Negreiros, D., Cerabolini, B. E., Kattge, J., Díaz, S., Kleyer, M., ... & Tampucci, D.
- 579 (2017). A global method for calculating plant CSR ecological strategies applied across biomes
- 580 world-wide. *Functional Ecology* 31, 444-457.
- 581
- 582 Ramirez, K.S., Snoek, L.B., Koorem, K. et al. (2019). Range-expansion effects on the
- 583 belowground plant microbiome. *Nature Ecology Evolution* 3, 604–611.
- 584
- 585 Reijenga BR, Murrell DJ, Pigot AL. (2021) Priority effects and the macroevolutionary dynamics
- 586 of biodiversity. *Ecology Letters* 24, 1455-1466.
- 587
- 588 Rivett, D.W., Bell, T. (2018). Abundance determines the functional role of bacterial phylotypes in
- 589 complex communities. *Nature Microbiology* 3, 767–772.
- 590
- 591 Rüger, N., Condit, R., Dent, D. H., DeWalt, S. J., Hubbell, S. P., Lichstein, J. W., ... & Farrior,
- 592 C. E. (2020). Demographic trade-offs predict tropical forest dynamics. *Science*, 368, 165-168.
- 593

594 Sanchez-Gorostiaga, A., Bajić, D., Osborne, M. L., Poyatos, J. F., & Sanchez, A. (2019). High-
595 order interactions distort the functional landscape of microbial consortia. *PLoS Biology*, 17,
596 e3000550.

597

598 Schmid, M. W., van Moorsel, S. J., Hahl, T., De Luca, E., Deyn, G. B., Wagg, C., ... & Schmid,
599 B. (2021). Effects of plant community history, soil legacy and plant diversity on soil microbial
600 communities. *Journal of Ecology* 109, 3007– 3023

601

602 Shahab, R. L., Brethauer, S., Davey, M. P., Smith, A. G., Vignolini, S., Luterbacher, J. S., & Studer,
603 M. H. (2020). A heterogeneous microbial consortium producing short-chain fatty acids from
604 lignocellulose. *SCIENCE*, 369(6507).

605

606 Spencer, H. G. (2020). Beyond Equilibria: The Neglected Role of History in Ecology and
607 Evolution. *The Quarterly Review of Biology*, 95, 311-321.

608

609 Strickland MS, Lauber C, Fierer N, Bradford MA (2009) Testing the functional significance of
610 microbial community composition. *Ecology* 90, 441–451.

611

612 Tedersoo, L., Bahram, M., Põlme, S., Kõljalg, U., Yorou, N. S., Wijesundera, R., ... & Smith, M.
613 E. (2014). Global diversity and geography of soil fungi. *SCIENCE*. DOI:
614 10.1126/science.1256688

615

- 616 Terrer, C., Phillips, R.P., Hungate, B.A. et al. (2021) A trade-off between plant and soil carbon
617 storage under elevated CO₂. *Nature* 591, 599–603
- 618
- 619 Tilman, D., Isbell, F., & Cowles, J. M. (2014) Biodiversity and ecosystem functioning. *Annual
620 Review of Ecology, Evolution, and Systematics*, 45, 471-493.
- 621
- 622 Thompson, L., Sanders, J., McDonald, D. et al. (2017). A communal catalogue reveals Earth's
623 multiscale microbial diversity. *Nature* 551, 457–463.
- 624
- 625 Thornton, M.M., R. Shrestha, Y. Wei, P.E. Thornton, S. Kao, and B.E. Wilson. 2020. Daymet:
626 Daily Surface Weather Data on a 1-km Grid for North America, Version 4. ORNL DAAC, Oak
627 Ridge, Tennessee, USA. <https://doi.org/10.3334/ORNLDAAC/1840>
- 628
- 629 Travisano, M., Mongold, J. A., Bennett, A. F., & Lenski, R. E. (1995). Experimental tests of the
630 roles of adaptation, chance, and history in evolution. *Science*, 267, 87-90.
- 631
- 632 Van Der Putten, W. H. (2017). Belowground drivers of plant diversity. *Science*, 355, 134-135
- 633
- 634 van der Plas, F., Schröder-Georgi, T., Weigelt, A. et al. (2020). Plant traits alone are poor
635 predictors of ecosystem properties and long-term ecosystem functioning. *Nature Ecology
636 Evolution* 4, 1602–1611.
- 637

- 638 Van Voris, P., O'Neill, R. V., Emanuel, W. R., & Shugart Jr, H. H. (1980). Functional complexity
639 and ecosystem stability. *Ecology*, 1352-1360.
- 640
- 641 Veen, G. F., Keiser, A. D., van der Putten, W. H., & Wardle, D. A. (2018). Variation in home-
642 field advantage and ability in leaf litter decomposition across successional gradients. *Functional
643 Ecology*, 32, 1563-1574.
- 644
- 645 Wang, B., & Allison, S. D. (2021). Drought legacies mediated by trait trade - offs in soil
646 microbiomes. *Ecosphere*, 12, e03562.
- 647
- 648 Wang, B., & Allison, S. D. (2019). Emergent properties of organic matter decomposition by soil
649 enzymes. *Soil Biology and Biochemistry*, 136, 107522.
- 650
- 651 Wang, B., Shuman, J., Shugart, H. H., & Lerdau, M. T. (2018). Biodiversity matters in feedbacks
652 between climate change and air quality: a study using an individual-based model. *Ecological
653 Applications*, 28, 1223-1231.
- 654
- 655 Watt, A. S. (1947). Pattern and Process in the Plant Community. *Journal of Ecology* 35, 1-22
- 656
- 657 Weemstra, M., Mommer, L., Visser, E. J., van Ruijven, J., Kuyper, T. W., Mohren, G. M., &
658 Sterck, F. J. (2016). Towards a multidimensional root trait framework: a tree root review. *New
659 Phytologist*, 211, 1159-1169.
- 660

- 661 Weigelt, A., Mommer, L., Andraczek, K., Iversen, C. M., Bergmann, J., Bruelheide, H., ... &
662 McCormack, M. L. (2021). An integrated framework of plant form and function: The belowground
663 perspective. *New Phytologist*. 232, 42–59
- 664
- 665 Weisskopf, L., Schulz, S., & Garbeva, P. (2021). Microbial volatile organic compounds in intra-
666 kingdom and inter-kingdom interactions. *Nature Reviews Microbiology*, 19, 391-404.
- 667
- 668 Westoby, M., Gillings, M. R., Madin, J. S., Nielsen, D. A., Paulsen, I. T., & Tetu, S. G. (2021).
669 Trait dimensions in bacteria and archaea compared to vascular plants. *Ecology Letters*. 24,1487–
670 1504.
- 671
- 672 Whitham, T. G., Bailey, J. K., Schweitzer, J. A., Shuster, S. M., Bangert, R. K., LeRoy, C. J., ...
673 & Wooley, S. C. (2006). A framework for community and ecosystem genetics: from genes to
674 ecosystems. *Nature Reviews Genetics*, 7, 510-523.
- 675
- 676 Wilson, D. S. (1997). Biological communities as functionally organized units. *Ecology*, 78, 2018–
677 2024.
- 678
- 679 Wilson RM, Zayed AA, Crossen KB, Woodcroft B, Tfaily MM, Emerson J, et al. (2021)
680 Functional capacities of microbial communities to carry out large scale geochemical processes are
681 maintained during ex situ anaerobic incubation. *PLoS ONE* 16: e0245857.
- 682

- 683 Wolf, A. A., Funk, J. L., Selmants, P. C., Morozumi, C. N., Hernández, D. L., Pasari, J. R., &
684 Zavaleta, E. S. (2021). Trait-based filtering mediates the effects of realistic biodiversity losses on
685 ecosystem functioning. *Proceedings of the National Academy of Sciences*, 118(26).
- 686
- 687 Wright, E., Vetsigian, K. (2016). Inhibitory interactions promote frequent bistability among
688 competing bacteria. *Nature Communications* 7, 11274
- 689
- 690 Yu, X., Polz, M.F. & Alm, E.J. (2019). Interactions in self-assembled microbial communities
691 saturate with diversity. *ISME J* 13, 1602–1617.
- 692
- 693 Zakem, E. J., Cael, B. B., & Levine, N. M. (2021). A unified theory for organic matter
694 accumulation. *Proceedings of the National Academy of Sciences* 118, e2016896118

Appendix

2

3 Climate-driven legacies in simulated microbial communities alter litter decomposition rates

4

5 Bin Wang^{1,2} and Steven Allison^{2,3}

6 1 Environmental Sciences Division, Oak Ridge National Laboratory, Oak Ridge, TN 37830 USA

7 2 Department of Ecology and Evolutionary Biology, University of California, Irvine, CA 92697

8 USA

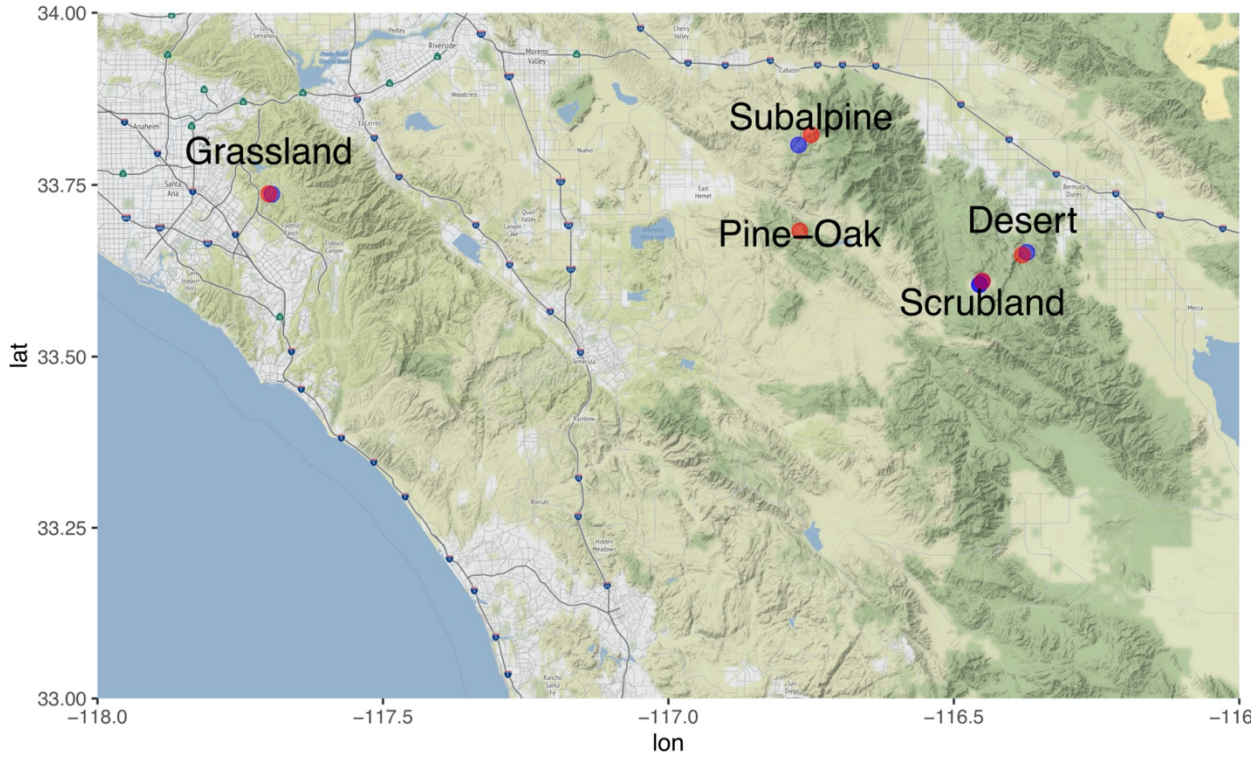
9 3 Department of Earth System Science, University of California, Irvine, CA 92697 USA

10

11 1. Gradient information

12 All five sites (**Supporting Fig. 1**) are located on granitic parent material and experience
13 Mediterranean precipitation patterns (cool, wet winters; hot, dry summers) with different
14 vegetation communities. The desert is dominated by desert perennials and annuals. The scrubland
15 is dominated by pinyon pine, juniper, and desert perennials and annuals. The grassland is
16 dominated by annual grasses and forbs, particularly *Bromus* and *Avena* spp. The pine-oak forest
17 is dominated by pines as well as evergreen and deciduous oak. The subalpine site is dominated by
18 lodgepole and limber pine.

19



20
21 **Supporting Fig. 1 Location of the five sites in Southern California, US.** Blue dots are nearby
22 eddy covariance flux tower sites (see <https://www.ess.uci.edu/~california/>). TAP (Total Annual
23 Precipitation; mm) = [213.5, 428.4, 569.4, 1415.8, 1376.5]. MAT (Mean Annual Temperature; °C)
24 = [22.8, 15.6, 16.4, 12.3, 10.3].

25
26 **2. DEMENTpy forcing**

27 **2.1 Average forcing**
28 One-year average forcing was approximated by leveraging the only litter water potential
29 data available at the grassland site, near Loma Ridge, California (**Allison and Goulden 2017**) and
30 field soil temperature measurements across the gradient (**Glassman et al. 2018**). Water potential
31 (ψ_{site} ; MPa) of the other four sites was derived by scaling the grassland site daily water potential
32 ($\psi_{grassland}$) of year 2011 (representative of typical annual conditions before the 2013 drought in

33 California) with Total Annual Precipitation (TAP; *mm*) and Mean Annual Temperature (MAT; °C)

34 at each site following:

35

$$36 \quad \psi_{site} = [1 + \ln\left(\frac{TAP_{grassland}}{TAP_{site}}\right) \frac{MAT_{site}}{MAT_{grassland}}] \psi_{grassland}$$

37

38 Soil temperatures at a sub-daily time step across the gradient at each of the five sites were measured.

39 From these field measurements, daily soil temperature was derived by averaging all measurements

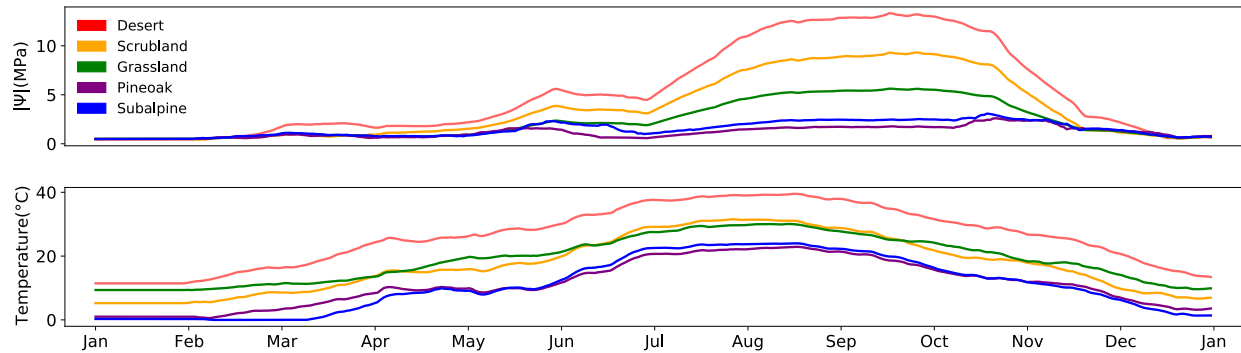
40 in each day. Details with regards to the measurement method, pre-, and post-processing are

41 documented in **Glassman et al. (2018)**. These data are openly accessible at

42 <https://github.com/stevenallison/UCIClimateExperiment/tree/master/updatednames>. Data derived

43 are further smoothed to get the eventual average forcing (**Supporting Fig.2**).

44



45

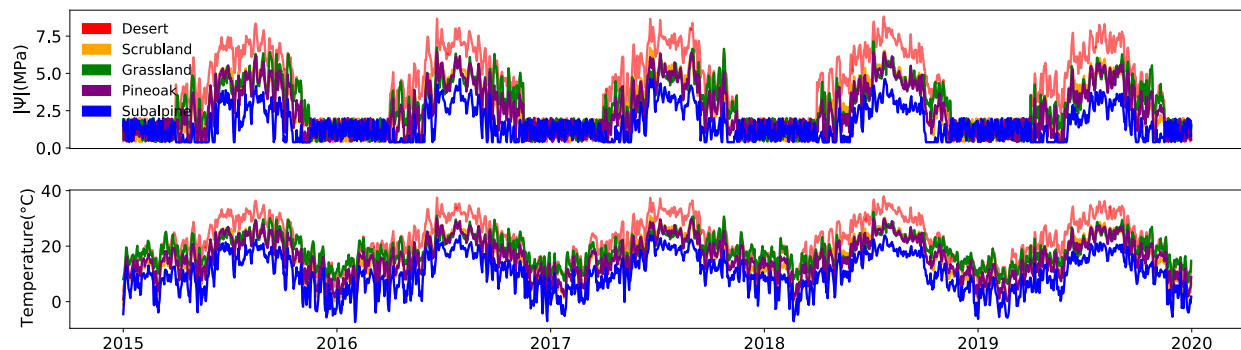
46 **Supporting Fig. 2 Average forcing of temperature and water potential.** This forcing was

47 recycled to equilibrate microbiomes at different sites.

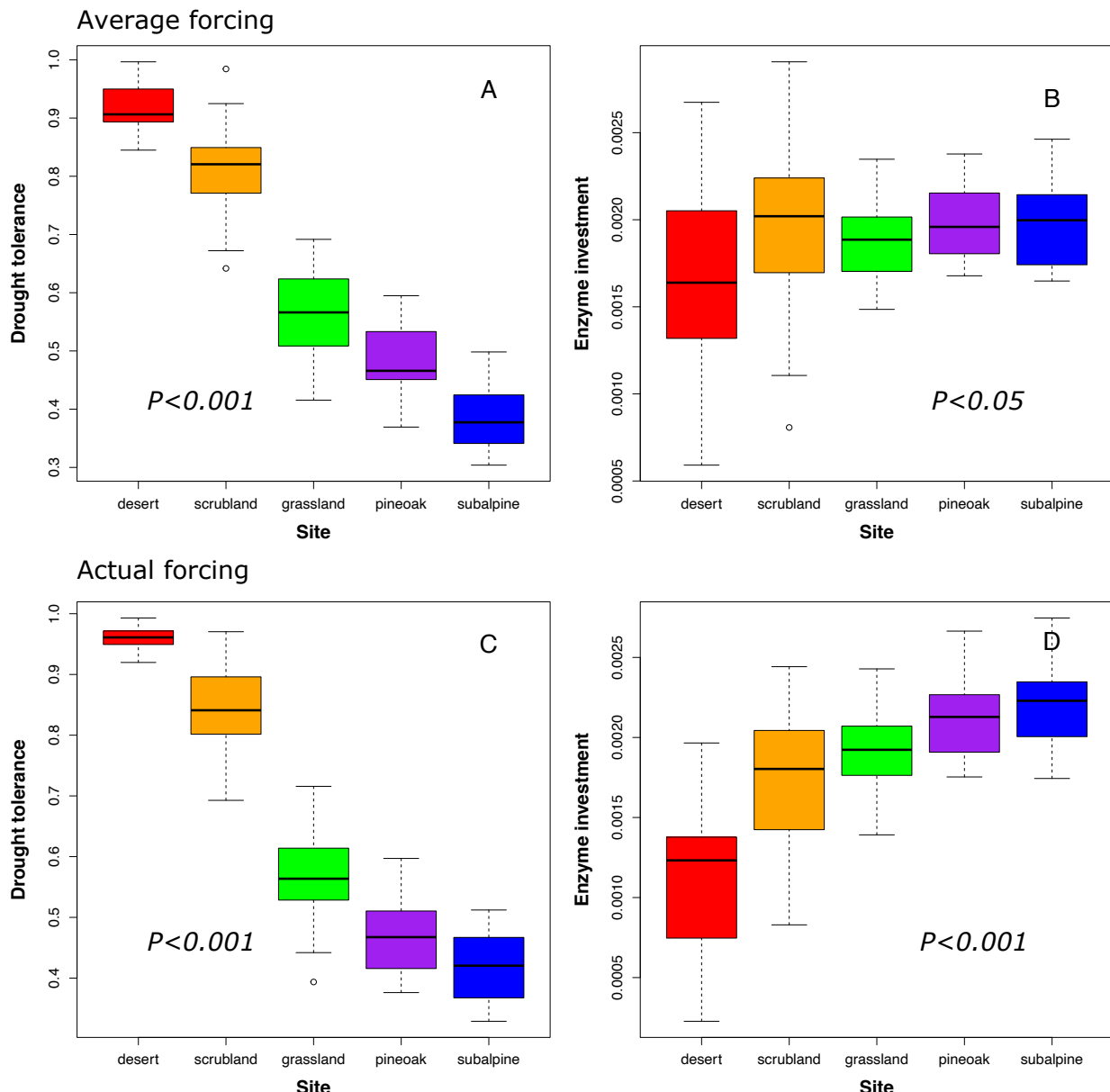
48

49 **2.2 Actual forcing**

50 Actual forcing follows the field transplant timeline (**Glassman et al. 2018**) to derive
51 forcing for 2015-2019. Daily soil surface temperature (°C) was from the Daymet (version 4;
52 **Thornton et al. 2020**) daily temperature product. Based on a machine learning framework, the
53 estimation of water potential fully leveraged all data available at the grassland site, near Loma
54 Ridge, California (2011-2013) including daily precipitation, field measurement of daily soil
55 surface temperature, and daily water potential derived from fuel moisture sensors (**Allison and**
56 **Goulden 2017**) to train a simple linear model. This trained model was then used to derive water
57 potential for each of the five sites from daily precipitation and air temperature data of 2015-2019
58 accessed from Daymet. The derived forcing is plotted in **Supporting Fig.3**.



59
60 **Supporting Fig. 3 Actual forcing from 2015 to 2019.** Note year 2015 was used after the 3-year
61 spin-up but before transplant.
62
63
64
65
66
67

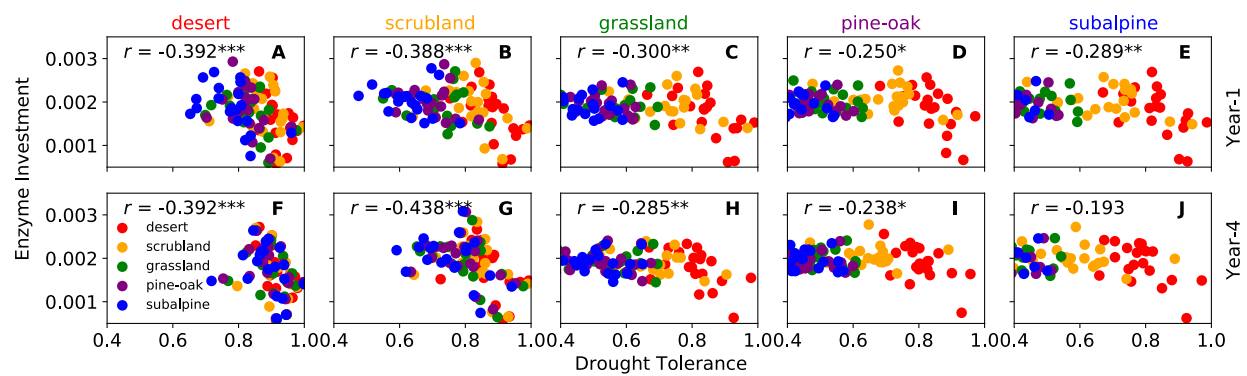


70 **Supporting Fig. 4 Microbial community traits (drought tolerance and enzyme investment;**
 71 **n=20) at the five sites across the gradient before transplant after spin-up under average**
 72 **forcing (A, B) and actual forcing (C, D).**

75

76

77



78

79 **Supporting Fig. 5 Correlations between enzyme investment and drought tolerance across the
80 gradient.** Significance code: $P < 0.001^{***}$, $P < 0.01^{**}$, and $P < 0.05^*$. Panels correspond
81 to sites and symbols correspond to community origin.

82

83

84

85

86

87

88

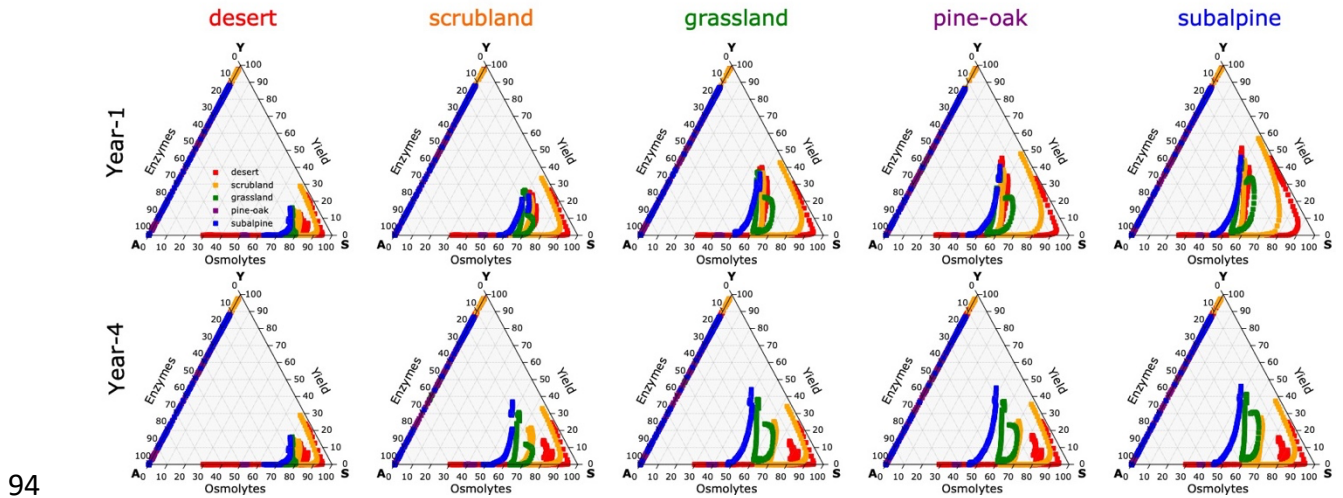
89

90

91

92

93



94 **Supporting Fig. 6 Ternary plots of community allocation among enzyme, osmolyte, and yield**
 95 **over the whole year.** Yield, enzymes, and osmolytes correspond to Y (Yield), A (resource
 96 Acquisition), and S (Stress), respectively. Points along the Y-A edge are low in osmolyte
 97 production in the wet season. At the desert site, from the 1st year through the 4th year, resource
 98 allocation among enzyme, osmolytes, and yield displayed little change (i.e., unchanged correlation
 99 strength); communities all had more allocation to osmolyte production by only differentiating
 100 along the A-S edge (i.e., stronger correlation between drought tolerance and enzyme investment
 101 as shown in **Supporting Fig. 5A, F**). At the grassland site, from the 1st through the 4th year the
 102 allocation pattern changed, with communities having higher yield (i.e., lower correlation strength;
 103 **Supporting Fig. 5C, H**) and communities differentiating not only along the A-S dimension (i.e.,
 104 correlation strength lower than the desert site). At the subalpine site, allocation by communities
 105 became more yield-driven from the 1st year through the 4th year (i.e., uncorrelated drought
 106 tolerance and enzyme investment as shown in **Supporting Fig. 5E, J**).
 107
 108